Morphology, Dynamic Mechanical Properties, and Gas Separation of Crosslinking Silica-Containing Polyimide Nanocomposite Thin Film

Mei-Hui Tsai,[1] Shih-Liang Huang,[1] Pei-Chun Chiang,[2] Chiou-Juy Chen[1]

[1]*Department of Chemical and Materials Engineering, National Chin-Yi University of Technology, Taichung 41111, Taiwan, Republic of China*
[2]*Department of Materials Science and Engineering, Mingdao University, ChangHua 52345, Taiwan, Republic of China*

Received 9 February 2007; accepted 14 May 2007
DOI 10.1002/app.26830
Published online 14 August 2007 in Wiley InterScience (www.interscience.wiley.com).

ABSTRACT: Silica-containing polyimide (PI-Si) crosslinked hybrid films are synthesized and applied to gas separation application. The PI-Si hybrid films are prepared from 4,4′-diaminodiphenyl ether (ODA), 3, 3′-oxydiphthalic anhydride (ODPA), *p*-aminophenyltrimethoxysilane (APTS), and phenyltrimetoxysilane (PTS). The monomer of monoamide APTS is used to modulate the block chain length of ODA–ODPA and then form bonding between PTS and ODA–ODPA phases. In the series of *x*ASPI (where *x* indicates the molecular weight (in kg/mol) of PI block chain length of ODA–ODPA and ASPI denotes PI modified with APTS) hybrid films, the glass transition temperature (T_g) increases and α-relaxation damping peak intensity decreases with the increase of APTS content. Meanwhile, the gas permeabilities of O_2 and N_2 of *x*ASPI films are slightly higher as compared with pure PI. The other series of (5AS–*y*-S)PI (5ASPI incorporates with PTS and *y* is the weight of PTS) hybrid films, the properties of T_g, density, and α-relaxation damping peak intensity are decreased with increasing the PTS content. However, higher O_2 and N_2 gas permeabilities and O_2/N_2 selectivity are achieved by increasing the PTS content in (5AS–*y*-S)PI hybrid films. © 2007 Wiley Periodicals, Inc. J Appl Polym Sci 106: 3185–3192, 2007

Key words: polyimide; nanocomposite; sol–gel; crosslink; gas separation

INTRODUCTION

Gas separation processes which use polymeric films have rapid improvement since 1980s. Membrane gas separations are energy saving processes and studies of membrane's structure and composition modification for high gas permeability and selectivity are well known for the industrial applications. The gas transport through polymeric materials is largely influenced by the differences in polymer chain's intrasegmental mobility and intermolecular attraction forces. The latter two phenomena are based on the changes of chemical structure, composition, and free volume of polymeric materials.[1–5]

Polyimide (PI) films possess many superior characteristics such as high mechanical strength, high temperature stability, chemical resistance, adhesion, ultrathin film formation, and high gas selectivity.[4–8] Many studies on the PI/inorganic hybrid and crosslinked material[9–21] for gas separation are of interest. Therefore, PIs with inorganic modifiers and crosslinks are synthesized for further improving high temperature resistance, mechanical strength, and intermolecular packing.[22–24] The reason for the better gas performance of crosslinked PI hybrid film compared to pure PI is because the microstructure of the former material can be adjusted by the variation of degree of crosslinking, which controls the free volume and hence used for the separation of a wide variety of gases. Many studies for the preparation of crosslinked PI use the UV-irradiation method.[25–28] The degree of crosslink depends on the irradiation time, intensity, or the type of mercury lamp. A disadvantage is that the UV-irradiation crosslink reaction often induces the nonhomogeneous irradiation between upper and under layer and the difficulty for controlling the crosslink density of film.

In this article, systematic studies for the silica-containing PI (PI-Si) crosslinked hybrid films are characterized with respect to the morphology, density, dynamic mechanical properties, and gas separation. Moreover, the correlation between gas separation performance and dynamic mechanical properties, density, and morphology are investigated as well.

Correspondence to: M. H. Tsai (tsaimh@ncut.edu.tw).
Contract grant sponsor: National Science Council of the Republic of China; contract grant numbers: NSC 91-2626-E-167-001, 93-2216-E-167-003.

Journal of Applied Polymer Science, Vol. 106, 3185–3192 (2007)

EXPERIMENTAL

Materials

3,3′-Oxydiphthalic anhydride (ODPA, 98%) from Tokyo Chemical Industry (Japan) is purified by recrystallization from acetic anhydride and then dried in a vacuum oven at 125°C over night. 4,4′-Diaminodiphenylether (ODA, 98%) from Lancaster is dried in a vacuum oven at 120°C for 3 h prior to use. *p*-Aminophenyltrimethoxysilane (APTS, 95% para and 5% meta) from Gelest Inc. and phenyltrimethoxysilane (PTS, 98%) from Lancaster are used as supplied. *N*-Methyl-2-pyrrolidone (NMP) from Tedia Company is dried over molecular sieves.

Preparation of films

Accurately measured amounts of ODA, APTS, and ODPA are added to the reactor and subsequently suitable amount of NMP (15 g) is added in series. Mixing thoroughly for 2 h at room temperature, aminophenyltrimethoxysilyl-terminated polyamic acid (APTS–PAA) oligomers with 25% (w/w) solid content is obtained. By controlling the amount of APTS, different molecular weights of PI, ODA–ODPA, block chain length from 3, 5, 10, to 20 kg/mol (designated as x = 3, 5, 10 and 20) of xASPI hybrid films are obtained. As in the preparation of the APTS–PAA with a PAA block molecular weight of 5000 g/mol, 1.225/1.0 mol ratio of ODPA/ODA is added into reaction vessel and then 0.45 mol ratio of APTS with respect to the former mole ratio in NMP solvent (for the solution with 25% solid content, w/w).

Then different amounts of 1.2, 3.5, and 5 g of PTS (designated as y values) are added to the above APTS–PAA solution of 5ASPI, respectively. After 15 h, the PAA–PTS homogeneous solutions with golden color are obtained under room temperature. The APTS–PAA and APTS–PAA–PTS solutions are coated on a PET film using a thickness of 250-μm knife coater. The films are first soft-baked at 60°C for 1 h in an air-circulating oven and then fixed in a rectangle stainless steel frame clamp and heated at the curing temperature of 100, 150, 200, and 300°C each for 1 h at atmospheric pressure in air. The obtained hybrid films from APTS–PAA and APTS–PAA–PTS solution are encoded as xASPI and (xAS–y-S)PI, respectively. Pure PI is synthesized from ODA and ODPA only. The dried hybrid films with thickness of 30–40 μm are subjected to the composition and property measurements. The APTS content decreases from 3ASPI to 20ASPI, which indicates that the PI block chain length of ODA–ODPA increases from 3, 5, 10, to 20 kg/mol. With increase in the PTS content increases from (5AS–1.2-S)PI, (5AS–3.5-S)PI, to (5AS–5.0-S)PI, which will form intermolecular crosslinks through sol–gel reaction between APTS and PTS, the crosslink density between PTS and APTS–PAA prepolymer increases. The reaction scheme and chemical structure of PI-Si hybrid films are presented in Scheme 1. The compositions of PI-Si hybrid films are shown in Table I.

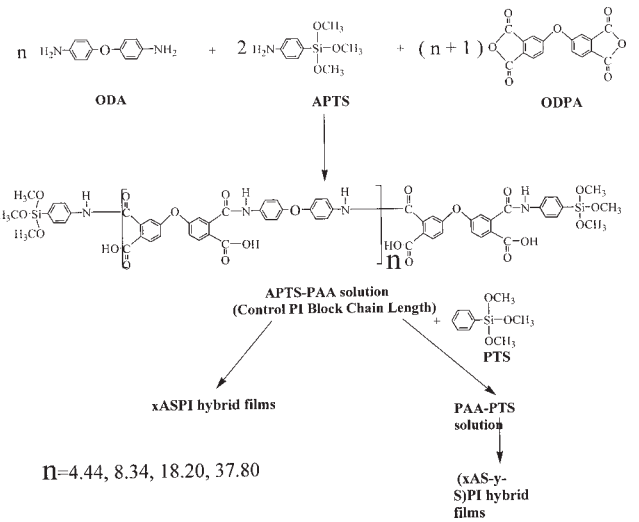

Scheme 1 Reaction scheme and chemical structure of PI-Si hybrid films.

Characterization and measurements

Infrared spectra are obtained using a Nicolet PROTEGE-460 Fourier transform infrared spectrophotometer (FTIR). Thermogravimetric analysis (TGA) is carried out with a TA Instrument 2950 at a heating rate of 10°C/min under nitrogen. The tested sample weighed about 10 mg. The glass transition temperature (tan δ peak) and dynamic mechanical properties are measured using a TA Instruments DMA 2980 dynamic mechanical analyzer at a heating rate of 3°C/min and 1 Hz from 60 to 330°C. The density of the hybrid film is measured by using an electronic densometer SD-120L with four pieces of the film, 3 × 3 cm each. The density data reported here are the averages of the four measurements values at 25°C. The sample for transmission electron microscope (TEM) analysis is prepared by putting (5AS–1.2-S) PI film into epoxy capsules first and then curing the epoxy at 70°C for 24 h in a vacuum oven. The hybrid-imbedded epoxy is microtomed with Leica Ultracut Uct into 90-nm-thick slices in a direction normal to the plane of the films. Subsequently, a layer of carbon of about 3 nm is deposited on the surface of each slice that is being placed on mesh 200 copper nets for TEM observation. TEM analysis was performed using JEOL-2000 FX with an acceleration voltage of 200 kV. Scanning electron microscope (SEM) is used to observe the cross section of the hybrid film. The sample is broken in liquid N_2. The

TABLE I
The Composition of APTS–PAA with 25% Solid Content in 15g of NMP Solvent

	Mole ratio[a] (g)			
Sample code	ODA	ODPA	APTS	PTS
3ASPI	1.0 (1.4802)	1.225 (2.8096)	0.45 (0.7102)	0 (0)
5ASPI	1.0 (1.6724)	1.120 (2.9011)	0.24 (0.4265)	0 (0)
10ASPI	1.0 (1.8171)	1.055 (2.9698)	0.11 (0.2131)	0 (0)
20ASPI	1.0 (1.8892)	1.0265 (3.0043)	0.053 (0.1065)	0 (0)
(5AS–1.2-S)PI	1.0 (1.6724)	1.120 (2.9011)	0.24 (0.4265)	0.7245 (1.2)
(5AS–3.5-S)PI	1.0 (1.6724)	1.120 (2.9011)	0.24 (0.4265)	2.1133 (3.5)
(5AS–5.0-S)PI	1.0 (1.6724)	1.120 (2.9011)	0.24 (0.4265)	3.0189 (5.0)
Pure PI	1.0 (1.9615)	1.0 (3.0385)	0 (0)	0 (0)

[a] Mole of ODA + mole of APTS × 1/2 = mole of ODPA.

apparatus used is Hitachi S4500 and specimen is precoated with a thin layer of gold.

Oxygen and nitrogen (mixing air) permeabilities of the hybrid films are determined by using the Yanaco GTR-10 gas permeability analyzer. The data of gas permeabilities are the average of at least three measurements. Experiments are carried out by measuring air gas flows through the membrane under constant transmembrane pressure of 38 cmHg. The gas permeation area is 15.6 cm^2; the gas permeability is evaluated using the following equation:

$$P = \frac{ql}{(P_1 - P_2)A}$$

where P is the N_2 or O_2 gas permeability [cm^3(STP) cm/(cmHg cm^2 s)], q is the volumetric flow rate of gas permeation [cm^3 (STP)/s], l is the film thickness(cm), P_1 and P_2 are the upstream and downstream pressures (cmHg), and A is the effective film area (cm^2).

RESULTS AND DISCUSSION

Characterization and properties of *x*ASPI Films

The synthesized PI-Si crosslinked hybrid films display homogeneous and transparent appearance, while 3ASPI film shows less flexibility as compared with other hybrid films. Because of the rigidity and brittleness of hybrid films, the series of 3ASPI hybrid films are ineligible for gas separation application. The other series of hybrid films are transparent and flexible and eligible for gas separation analysis.

Infrared spectra of pure PAA and pure PI film are shown in Figure 1(a,b). It can be seen that the characteristic absorption peaks of PI are clearly presented: the imide absorption peaks are 1780 cm^{-1} for C=O asymmetrical stretching, 1720 cm^{-1} for C=O symmetrical stretching, and 1380 cm^{-1} for C—N stretching. The increase of the absorption band at 1110–1140 cm^{-1} is due to Si-O-Si band formation of (5AS–3.5-S) PI hybrid film, as shown in Figure 1(c). The absorption intensity at 3200–3500 cm^{-1} of PAA decreased with the increase in imidization temperature and then disappeared for pure PI film, which can be regarded as well imidized.

All the *x*ASPI hybrid films possess superior thermal properties than have pure PI, shown in Table II. The 5% weight loss temperature of pure PI under nitrogen atmosphere is 527°C; however, the 5% weight loss temperature of the hybrid films starts at 550°C. All the *x*ASPI hybrid films also have a higher weight residue than the pure PI at 800°C. The considerable increase in thermal stability and char yield could be related to the addition of APTS. The moiety of silicon is increased and crosslink network structure is formed by adding APTS into PI. These results show improvement of the thermal properties of hybrid film and increase in the char yield as well.

Figures 2(a) and 3(a) show the storage modulus and tan δ as a function of temperature curves and T_g values for the pure PI and *x*ASPI hybrid films. For different PI block chain lengths of *x*ASPI hybrid films, the 5ASPI hybrid film with shorter PI block chain length possesses higher storage modulus, higher T_g values. The purpose of the addition of APTS for the PI synthesis is to control the block

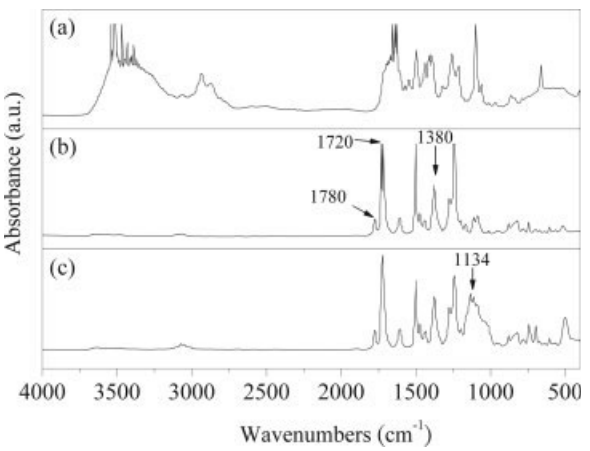

Figure 1 FTIR spectra of (a) pure PAA, (b) pure PI, (c) (5AS–3.5-S)PI.

TABLE II
Density and Thermal Properties of Pure PI, *x*ASPI, and (5AS–*y*-S)PI Hybrid Films

	Characteristics			
	TGA (N_2) (°C)			
Sample	5% weight loss	800°C Char (%)	DMA tan δ peak (T_g, °C)	Density (g/cm^3)
3ASPI	550	59.7	289	—[a]
5 ASPI	566	61.7	287	1.364
10 ASPI	570	62.7	284	1.369
20 ASPI	558	60.3	277	—
5 ASPI	566	61.7	287	1.364
(5AS–1.2-S)PI	558	64.0	283	1.352
(5AS–3.5-S)PI	563	66.4	279	1.335
(5AS–5.0-S)PI	570	69.5	277	1.334
Pure PI	527	58.3	271	1.368

[a] Not determined.

chain length of ODPA–ODA, which is a rigid segment in PI chain, and then intermolecular crosslink will occur between —Si(OCH$_3$)$_3$ groups of APTS by sol–gel reaction. The —Si—O—Si— crosslink structures are then formed through the sol–gel reaction between —Si(OCH$_3$)$_3$ groups to take off water. The increase of APTS content will decrease the ODPA–ODA block chain length and increase the intermolecular crosslinked density. 5ASPI is synthesized with higher APTS component than that for 10ASPI and 20ASPI films. 5ASPI possesses lower block chain length and higher crosslinked density in comparison

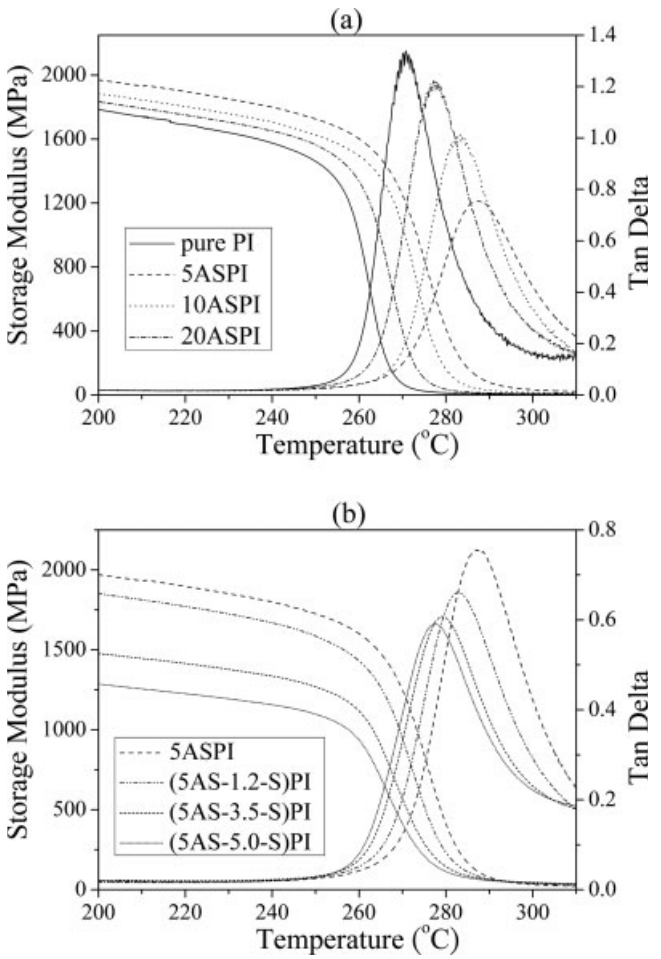

Figure 2 Dynamic mechanical properties of pure PI, 5ASPI, 10ASPI, and (5AS–3.5-S)PI.

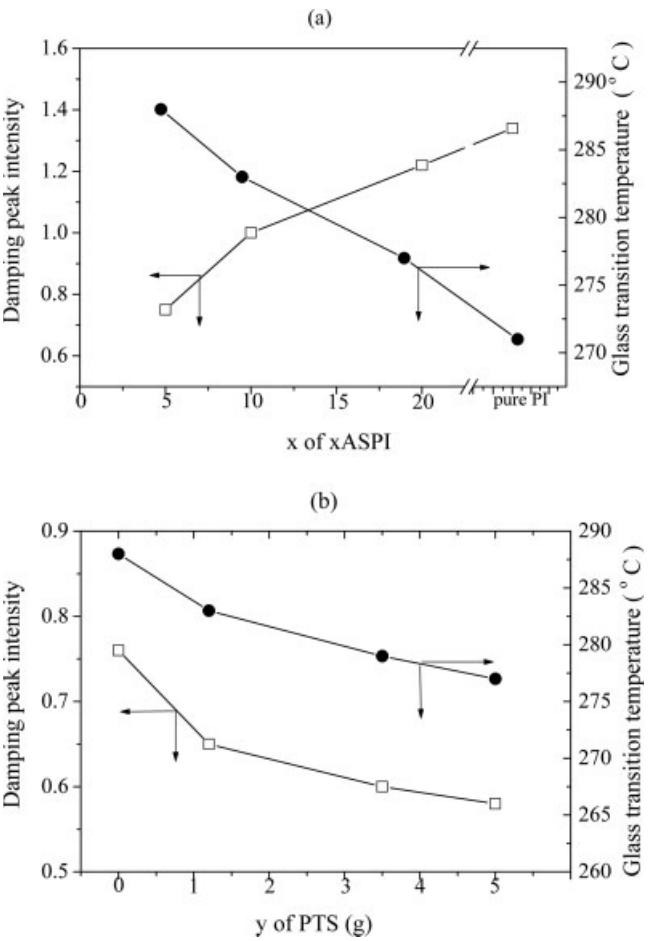

Figure 3 Glass transition temperature and damping peak intensity of (a) pure PI and *x*ASPI and (b) (5AS–*y*-S)PI.

to 10ASPI and 20ASPI films. This is the reason why 5ASPI film possesses the highest T_g and storage modulus among these three polymers.

On the other hand, polymer with rigid ODPA–ODA segment and more crosslinkage will induce the decrease of damping intensity. Figure 3(a) shows the effect of PI block chain length on damping intensity, which can be used to realize the molecular microphase structure. Damping may have resulted from polymer chain friction during chain movement, caused by intermolecular chain interaction. Therefore, low damping in the tan δ curve indicates a lower interaction force between molecular chains, and a high damping indicates high chain interaction force.[30] Figure 3(a) shows that the pure PI film possesses the lowest T_g value and the highest damping intensity as compared with *x*ASPI hybrid films. The longer the PI block chain length is the lower is crosslink density and higher is the induced damping strength of the hybrid film; the tan δ value indicates the damping intensity of the hybrid film. Low damping intensity of 5ASPI hybrid film displays smaller intermolecular attraction force and α-relaxation activation energy of hybrid films.

Figure 4(a,b) shows the effect of operating temperature on O_2 permeabilities and O_2/N_2 selectivity of pure PI and *x*ASPI hybrid films. The O_2 and N_2 permeabilities are found to increase with increasing operating temperature and follow Arrhenius behavior. In the *x*ASPI series, a tendency that all *x*ASPI hybrid films show higher O_2 permeabilities than do pure PI at low or elevated temperature was observed. 5ASPI hybrid film shows slightly higher O_2 permeability than does the other polymers for the *x*ASPI series. There are two factors affecting the free volume of polymer film: (1) the block chain length of ODA–ODPA and (2) the crosslink density. The decrease of block chain length will decrease the free volume between polymer chains and hence decrease the gas permeability. The increase in APTS content will increase the number of crosslink point, which is rigid segment of ODA–ODPA prop up the polymer chain; thus the free volume between polymer chains and gas permeability is slightly increased. *x*ASPI hybrid film with 5 kg/mol possesses the lowest block chain length and highest crosslink point density. The competition of above two contradictory effects indicates that the latter possesses superior influence on the gas permeability. This may result in the slightly higher gas permeability for the 5ASPI film compared with the other two polymers.

Figure 4(b) shows the O_2/N_2 selectivity decrease with the increase of operating temperature. Within the operating temperature range, the values of O_2/N_2 selectivity for pure PI and *x*ASPI show little difference. At 55°C, the O_2/N_2 selectivity of *x*ASPI hybrid films remains above 5.88. The value of

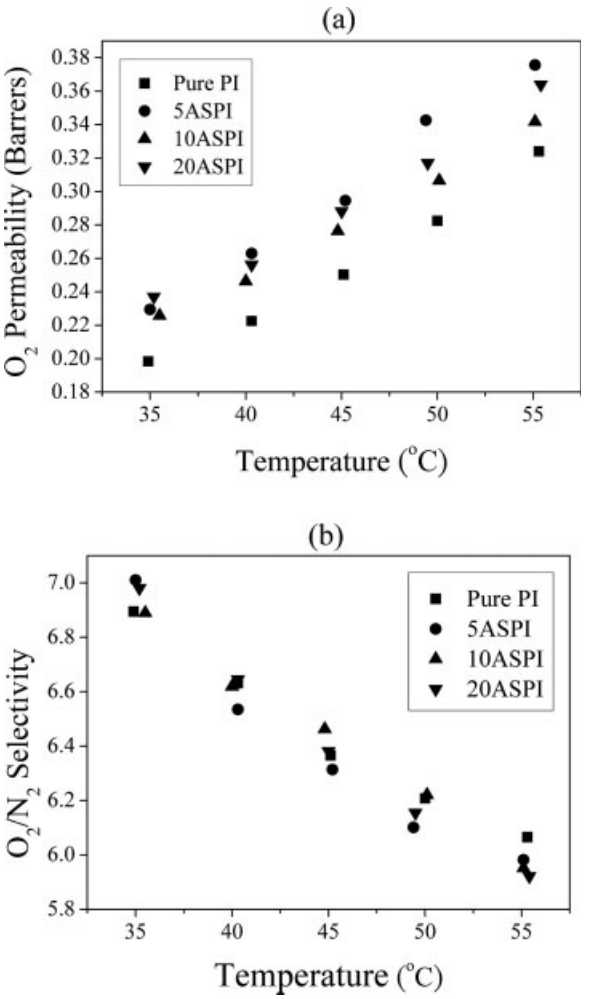

Figure 4 (a) O_2 permeability coefficients and (b) O_2/N_2 selectivity as a function temperature for pure PI and *x*ASPI.

O_2/N_2 selectivity depends on the affinity of polymer film with O_2 or N_2 gas, as the molecular sizes of O_2 and N_2 gases are nearly same. While 5ASPI polymer, which possesses more APTS content, contains —Si—O— group and is affinitive to O_2 gas, most of the —Si—O— groups of APTS are distributed in the bulk of film. Hence the O_2/N_2 selectivity of 5ASPI film, which possesses higher APTS content, will be higher than that of the other two films. Whereas 5ASPI film posseses larger free volume as discussed in the former section, the O_2/N_2 selectivity of 5ASPI film will be lower than that of the other two films. Consequently, the competition of the above two effects may be the reason for the O_2/N_2 selectivities of three *x*ASPI films are nearly the same.

Characterization and properties of (5AS–*y*-S)PI Films

The absorption intensity at 3200–3500 cm^{-1} of PAA decreased as the increase of imidization temperature and then disappeared for (5AS–3.5-S)PI hybrid film

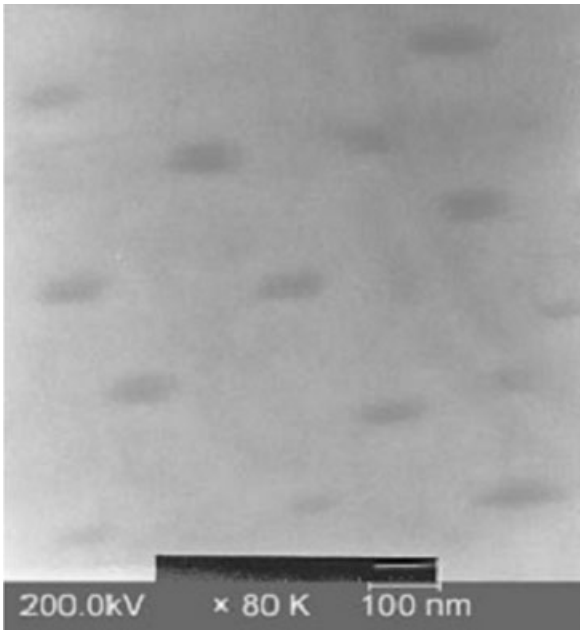

Figure 5 TEM images of (5AS–1.2-S)PI.

as shown in Figure 1. The peak of 1134 cm^{-1} representing the formation of the Si—O—Si crosslink structure is also observed for the (5AS–3.5-S)PI hybrid film.

The TEM analysis of the (5AS–1.2-S)PI hybrid film is shown in Figure 5. According to TEM data, the particle size of silica is in the range from 80 to 100 nm and well distributed in PI matrix. Figure 6 demonstrates the SEM images of the silica nano domain size of 50–80 nm for (5AS–1.2-S)PI film, 50–150 nm for (5AS–3.5-S)PI film, and 100–200 nm for (5AS–5.0-S) PI film. The (5AS–1.2-S)PI hybrid film exhibits smoother and denser morphology in comparison with (5AS–3.5-S)PI and (5AS–5.0-S)PI hybrid films. The former shows some voids in the structure and rougher morphology, the latter shows the most obvious roughness and biggest cavity. It is suggested that the size of silica domain and pore structure increase with increasing the PTS content. This result will influence the property of gas transportation as discussed in the following section.

As shown in Table II, the pure PI shows that the 5% weight loss temperature is at 527°C under nitrogen, however, the 5% weight loss temperature of the hybrid films starts at 550°C. The (5AS–*y*-S)PI hybrid films also have a higher weight residue than pure PI at 800°C. The considerable increase in thermal stability and char yield could be related to the addition of APTS and PTS. The moiety of silicon is increased and crosslink network structure is formed by adding APTS and PTS into PI. These results improve the thermal properties of hybrid film and increase char yield as well.

The densities of hybrid films are measured and may be used as a collateral evidence for the change of free volume contained in the hybrid films. Table II shows the dependence of the densities of PI-Si hybrid films on the various PTS content. It is indicated that the density of the (5AS–*y*-S)PI films decreases with the PTS content. It may be suggested that the free volume of the hybrid films are increased with increasing the PTS content. A higher PTS content can cause larger silica domain size and

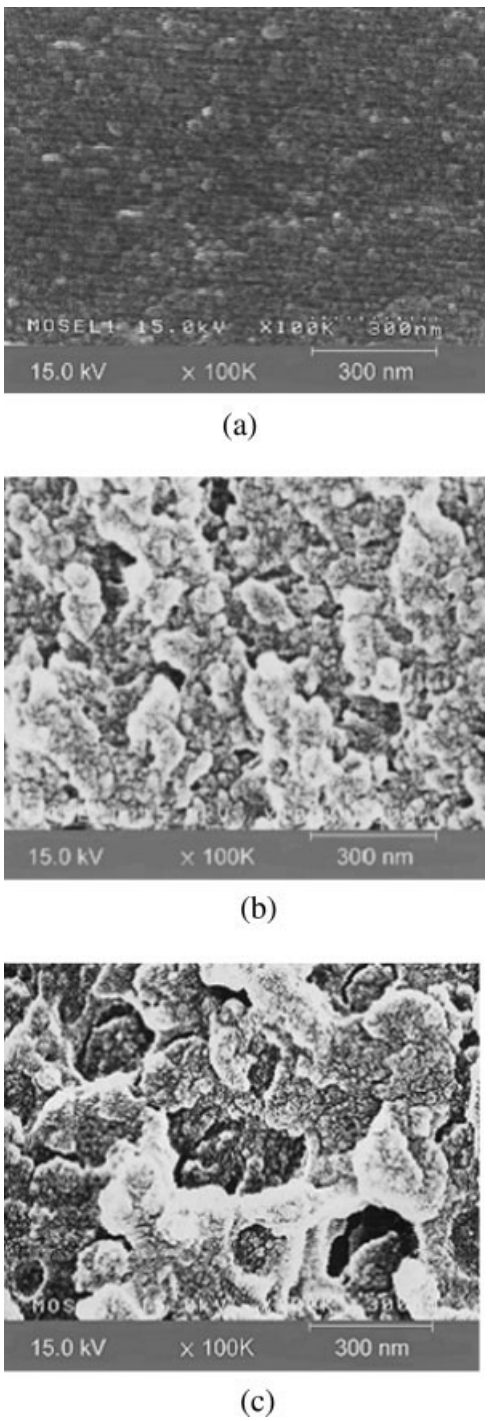

Figure 6 SEM images of the fracture surfaces of (a) (5AS–1.2-S)PI, (b) (5AS–3.5-S)PI, (c) (5AS–5.0-S)PI.

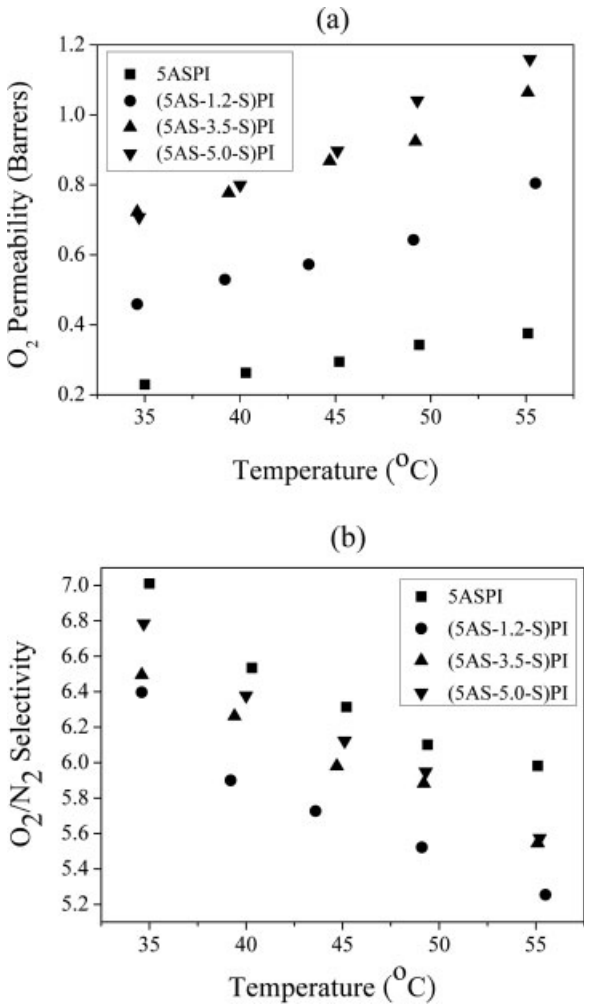

Figure 7 (a) O_2 permeability coefficients and (b) O_2/N_2 selectivity as a function temperature for 5ASPI and (5AS–*y*-S)PI.

microporous hybrid films, and lead to more free volume and a lower dielectric constant[29] in the hybrid films. The increase of free volume also may be investigated by the density changes from 1.364, 1.3520, 1.3350, and 1.3341 g/cm^3 for 5ASPI, (5AS–1.2-S)PI, (5AS–3.5-S)PI, and (5AS–5.0-S)PI, respectively.

In the series of (5AS–*y*-S)PI hybrid films, DMA curves show that introducing PTS into the 5ASPI hybrid structure to form greater silica domains and then the storage modulus and T_g decreased [see Figs. 2(b) and 3(b)]. Figure 3(b) shows that damping intensity and T_g both decrease with the increase of PTS content for (5AS–*y*-S)PI hybrid films. The main reason is that films containing PTS will produce larger size of silica phase domain, which will produce obvious interface porosity as shown by SEM and TEM graphs in Figure 5 and 6. Meanwhile, these PTS will increase the polymer chain length (i.e., final polymer weight), which changes to more flexible. This will decrease the damping intensity and T_g value with the increase in PTS content.

Figure 7(a) indicates the O_2 permeabilities of (5AS–*y*-S)PI hybrid films. It is seen that the permeability properties of O_2 are obviously increased as PTS content increased. At 55°C, the O_2 permeability values of (5AS–5.0-S)PI hybrid film are 1.19 barr, which are 3.7 times higher than that of pure PI (P_{O_2} = 0.32 barr). The reason is that the increase of PTS content will increase the silica domain, free volume, and gas permeability while the O_2/N_2 selectivities of (5AS–*y*-S)PI series are all lower than that of pure PI. It deserves to be mentioned that as the increase of PTS content for (5AS–*y*-S)PI hybrid film will increase both O_2 and N_2 permeabilities and O_2/N_2 selectivity. From the SEM graph, it can be seen that (5AS–*y*-S)PI hybrid film, which has higher content, possesses larger porosity and lower density. These two phenomena mean the free volume of film and that is the reason for the increase of gas permeability while the O_2/N_2 selectivity of (5AS–*y*-S)PI hybrid film increase as the increase of PTS content. The main reason may be that larger absorption and diffusion are formed between silica element and O_2.[10,31] Then the increase of PTS content will increase more O_2 permeability more than N_2 gas and hence the O_2/N_2 selectivity increased. The other contribution for the crosslinked structure to hybrid film is that the restriction of the plasticization of PI chain, leading to prevent the large decrease of the gas selectivity.[32] The O_2 and N_2 permeability of (5AS–5.0-S)PI hybrid film are all nearly 3.5–4.2 times higher than in pure PI film. Meanwhile, the O_2/N_2 selectivity is less 12% lower than pure PI film and remains at above 5.25.

CONCLUSIONS

The gas separation, morphology, and dynamic mechanical properties of PI-Si hybrid films are studied. A simpler method of preparing the PI-Si hybrid films has been developed by sol–gel processes. The silica domains are fairly homogeneously dispersed in the range 50–200 nm in the hybrid films by both TEM and SEM observation. In the series of *x*ASPI hybrid film, the higher content of APTS is incorporated, the higher crosslink structure of the hybrid film is formed. Besides, the crosslink structure of the *x*ASPI hybrid film will reinforce the pure PI. While for the gas separation performances, the results have not obvious and distinct differences among these hybrids. In the series (5AS–*y*-S)PI films, the T_g, tan δ peak intensity, density decrease, and silica domains, O_2 and N_2 gas permeabilities increase with PTS content. It seems that a with more silica structure in the hybrid films leads to more free volume or greater interblock separation. For the hybrid film with (5AS–*y*-S)PI, as the PTS content increases, O_2/N_2 selectivity is also increased. It may be that larger affinity

formed between Si element and O_2 and the crosslink structure of hybrid films for the higher O_2/N_2 selectivity as compared with pure PI.

References

1. Stern, S. A. J Membr Sci 1994, 94, 1.
2. Ackern, F. V.; Lutz, K.; Bernd, T. Thin Solid Films 1998, 327, 762.
3. Andreeva, D. V.; Brozová, Z.; Bleha, M.; Polotskaya, G. A.; Elyashevich, G. K. Thin Solid Films 2002, 406, 54.
4. Chen, S. H.; Yu, K. C.; Huang, S. L.; Lai, J. Y. J Membr Sci 2000, 173, 99.
5. Huang, S. L.; Lai, J. Y. J Appl Polym Sci 1997, 64, 1235.
6. Ghosh, M. K.; Mittal, K. L.; Polyimides: Fundamentals and Applications; Marcel Dekker: New York, 1996.
7. Tsai, M. H.; Chiang, P. C.; Whang, W. T.; Ko, C. J.; Huang, S. L. Surf Coat Technol 2006, 200, 3297.
8. Okamoto, K.; Noborio, K.; Hao, J.; Tanaka, K.; Kita, H. J Membr Sci 1997, 134, 171.
9. Smaihi, M.; Schrotter, J. C.; Lesimple, C.; Prevost, I.; Guizard, C. J Membr Sci 1999, 161, 157.
10. Chen, S. H.; Lee, M. H.; Lai, J. Y. Eur Polym Mater 1996, 32, 1403.
11. Li, D.; Hwang, S. T. J Membr Sci 1992, 66, 119.
12. Hibshman, C.; Cornelius, C. J.; Marand, E. J Membr Sci 2003, 211, 25.
13. Cornrliu C., Hibshman C., Marand, E. Sep Purif Technol 2001, 25, 181.
14. Cornelius, C. J.; Marand, E. J Membr Sci 2002, 202, 97.
15. Park, H. B.; Lee, Y. M. Adv Mater 2005, 17, 477.
16. Bickel, C. S.; Koros, W. J. J Membr Sci 1999, 155, 145.
17. Fang, J.; Kita, H.; Okamoto, K. I. J Membr Sci 2001, 182, 245.
18. McCaig, M. S.; Paul, D. R. Polymer 1999, 40, 7209.
19. Marek, M.; Brynda, E.; Pientka, Z.; Schauer, J. Eur Polym Mater 1997, 33, 1717.
20. Tsai, M. H. Huang, S. L.; Muti Lin, J. C.; Ko, C. J.; Chen, Y. L.; Lu, C. M.; Chen, C. J.; Yen, C. H. J Appl Polym Sci, to appear.
21. Liu, Y.; Pan, C.; Ding, M.; Xu, J. Eur Polym Mater 1999, 35, 1739.
22. Tsai, M. H.; Ko, C. J. Surf Coat Technol 2006, 201, 4367.
23. Tsai, M. H.; Liu, S. J.; Chiang, P. C. Thin Solid Films 2006, 515, 1126.
24. Tsai, M. H.; Whang, W. T. J Polym Res 2001, 8, 77.
25. Kita, H.; Inada, T.; Tanaka, K.; Okamoto, K. J Membr Sci 1994, 87, 139.
26. Wright, C. T.; Paul, D. R. J Membr Sci 1997, 124, 161.
27. Matsui, S.; Nakagawa, T. J Appl Polym Sci 1998, 67, 49.
28. Matsui, S.; Nakagawa, T.; Higuchi, A. J Polym Sci Part B: Polym Phys 1997, 35, 2259.
29. Tsai, M. H.; Whang, W. T. Polymer 2001, 42, 4197.
30. Tsai, M. H.; Whang, W. T. J Appl Polym Sci 2001, 81, 2500.
31. Suzuki, T.; Yamada, Y. J Polym Sci Part B: Polym Phys 2006, 44, 291.
32. Park, H. B.; Kim, J. K.; Nam, S. Y.; Lee, Y, M, J Membr Sci 2003, 220, 59.